First-principles studies of intrinsic point defects in magnesium silicide

2009 J. Phys.: Condens. Matter 21 205801

(http://iopscience.iop.org/0953-8984/21/20/205801)

J. Phys.: Condens. Matter **21** (2009) 205801 (7pp) doi:10.1088/0953-8984/21/20/205801

First-principles studies of intrinsic point defects in magnesium silicide

Akihiko Kato, Takeshi Yagi and Naoto Fukusako

FDK Corporation, 2281 Washizu, Kosai, Shizuoka, Japan

E-mail: kato@fdk.co.jp

Received 4 November 2008, in final form 12 March 2009
Published 24 April 2009
Online at stacks.iop.org/JPhysCM/21/205801

Abstract

We have studied intrinsic point defects in magnesium silicide, Mg_2Si, by density-functional theory. Evaluating the formation energies of point defects, we show that n-type electric conductivity of Mg_2Si originates from formations of positively charged Mg ions at interstitial sites, regardless of the chemical composition in crystal growth. Moreover, we have calculated the Born effective charge tensors and the valence charge density distribution. They show Mg_2Si is an ionic crystal composed of Mg^{2+} and Si^{4-} which have very different ionic radii, 0.6 Å and 2.1 Å, respectively. We have concluded that the unfavorable antisite defect, Mg_{Si}, is due to the dissimilar ionic radii.

1. Introduction

Magnesium silicide, Mg_2Si, has attracted lots of interest as an environmentally friendly thermoelectric semiconductor [1–4] as it consists of elements that are non-toxic and abundant in nature. The Mg–Si phase diagram shows that Mg_2Si is the only compound in this system and it melts at 1358 K. Therefore crystal growth from the melt is possible, but a considerable amount of Mg tends to evaporate from the surface [5, 6] because the boiling temperature (1363 K)is close to the melting temperature and the vapor pressure of Mg is high. Quite naturally, an Mg vacancy, V_{Mg}, would be considered as a major defect in the crystal. In general, vacancies of cations tend to act as acceptors and to generate holes in the valence bands; semiconductors with such vacancies would exhibit p-type conductivities.

Contrary to such an expectation, undoped Mg_2Si exhibits n-type conductivity [1, 7, 8] under any chemical conditions in crystal growth, whereas an isomorphic compound, Mg_2Ge, reveals p-type (n-type) conductivity under Ge-rich (Mg-rich) conditions [9].

The discrepancy should be solved by detailed quantitative investigation of intrinsic defect formations in Mg_2Si. Aside from complex defects, the candidates for donor-like defects are positively charged, such as Mg at an interstitial site, Mg_i, antisite-Mg, Mg_{Si} or an anion vacancy, V_{Si}. However, no studies have elucidated the origin of the n-type conductivity of undoped Mg_2Si [10].

A recent first-principles calculation scheme has high reliability for predicting defect formations taking into account crystal growth conditions [11, 12]. The scheme does not deal with the dynamics of defect generation processes, but supposes thermodynamic equilibrium conditions. Sufficiently high mobilities of the atoms in the crystal are required so that defect formations equilibrate thermodynamically at the temperatures of interest. Fortunately, Mg_2Si can be considered as a material which satisfies the requirement because it can be fabricated owing to the high mobility of Mg [13, 14].

The aim of the present work is to elucidate the origin of the persistent n-type conductivity of Mg_2Si by means of first-principles analysis. We studied intrinsic point defect formations in Mg_2Si by density-functional theory. Evaluating the formation energies of all kinds of point defects in variously charged states, we show that the positively charged Mg_i is the most energetically stable defect under both Si-rich and Mg-rich conditions. It acts as an donor, $Mg_i \rightarrow Mg_i^{q+} + qe^-$, this is consistent with the persistent n-type conductivities in earlier experimental results [1, 7, 8].

This paper is organized as follows: in section 2 we make a brief review of the calculation method; in section 3 we present the numerical results and elucidate the origin of the n-type conductivity and the bonding character of Mg_2Si; our conclusions are given in section 4.

2. Calculation method

The calculated results we present throughout this work were produced by our first-principles electronic structure calculation program [15] in a pseudopotential scheme with plane-wave

basis functions. It provides electronic structures within density-functional theory (DFT) [16]. We employed dual-space Gaussian pseudopotentials (norm conserving) and an exchange–correlation functional (local-density approximation) with the parameters tabulated in reference [17].

Magnesium silicide belongs to the antifluorite structural type with an fcc cubic lattice, and the space group is $Fm\bar{3}m$. The unit-cell structure consists of Si ions occupying four lattice points (**4a**) and Mg ions occupying eight tetrahedral sites (**8c**). In addition, the structure has four equivalent interstitial sites (**4b**).

2.1. Defect formation energies and carrier concentrations

We determined the optimized lattice constant for the perfect crystal and kept it in all point defect calculations to eliminate spurious stresses [12]. We employed a periodic supercell system, though the defect formation energy should be the energy required to generate a single isolated defect in an infinite perfect crystal under a relevant crystal growth condition. If volume relaxation processes are carried out in defect calculations, the total energies would correspond to the ones for the bulk systems containing ordered arrays of defects at high concentrations. That is why the optimized lattice constant for the perfect crystal is employed in all defect calculations [12].

To evaluate defect formation energies, we adopted a well-established formalism [11, 12], which gives us the following formation energy, $E_{\rm f}^{\rm d}$, for a defect d, as a function of the chemical potentials of the constituent elements, $\mu_{\rm Mg}$, $\mu_{\rm Si}$, and an electron Fermi energy, $\epsilon_{\rm F}$, under a relevant crystal growth condition,

$$E_{\rm f}^{\rm d}(\mu_{\rm Mg}, \mu_{\rm Si}, \epsilon_{\rm F}) = E_{\rm tot}^{\rm d}(q_{\rm d}) - n_{\rm Mg}^{\rm d}\mu_{\rm Mg} - n_{\rm Si}^{\rm d}\mu_{\rm Si} + q_{\rm d}\epsilon_{\rm F}, \quad (1)$$

where $n_{\rm Mg}^{\rm d}$ and $n_{\rm Si}^{\rm d}$ are the numbers of Mg and Si atoms, respectively, in the supercell with the defect d; $q_{\rm d}$ is the charge state of the defect. The first term on the right-hand side of equation (1) is the total energy of the supercell system with the defect in charge state, $q_{\rm d}$.

Chemical potentials, $\mu_{\rm Mg}$ and $\mu_{\rm Si}$, depend on the chemical compositions under which the Mg_2Si crystal is grown. In thermodynamically equilibrium conditions, they are not independent since both species are in equilibrium with bulk Mg_2Si;

$$\begin{aligned}\mu_{\rm Mg_2Si} &= 2\mu_{\rm Mg} + \mu_{\rm Si} \\ &= 2\mu_{\rm Mg}^{\rm bulk} + \mu_{\rm Si}^{\rm bulk} - \Delta H_{\rm f}^{\rm Mg_2Si},\end{aligned} \quad (2)$$

where $\mu_{\rm Mg_2Si}$ is the total energy for the perfect crystal by means of the chemical formula. The chemical potentials for the elemental materials, $\mu_{\rm Mg}^{\rm bulk}$ and $\mu_{\rm Si}^{\rm bulk}$, are the total energies per atom in Mg (*hcp*) and Si (*diamond*) pure bulk crystals, respectively, and $\Delta H_{\rm f}^{\rm Mg_2Si}$ is the heat of formation.

Since Mg_2Si is the only compound in the Mg–Si system, no segregations, except for Mg_2Si, should be obtained if the boundary relations, $\mu_{\rm Mg} < \mu_{\rm Mg}^{\rm bulk}$ and $\mu_{\rm Si} < \mu_{\rm Si}^{\rm bulk}$, are satisfied. To sum up these conditions, we have the following expressions [18, 19],

$$\mu_{\rm Mg}^{\rm min} = \mu_{\rm Mg}^{\rm bulk} - \tfrac{1}{2}\Delta H_{\rm f}^{\rm Mg_2Si} < \mu_{\rm Mg} < \mu_{\rm Mg}^{\rm bulk}, \quad (3a)$$

$$\mu_{\rm Si}^{\rm min} = \mu_{\rm Si}^{\rm bulk} - \Delta H_{\rm f}^{\rm Mg_2Si} < \mu_{\rm Si} < \mu_{\rm Si}^{\rm bulk}. \quad (3b)$$

From equation (2), one free parameter characterizes the chemical composition in the crystal growth. For example, $\mu_{\rm Si}$ and $\mu_{\rm Mg}$ under Si-rich (Mg-rich) conditions are $\mu_{\rm Si}^{\rm bulk}$ ($\mu_{\rm Si}^{\rm min}$) and $\mu_{\rm Mg}^{\rm min}$ ($\mu_{\rm Mg}^{\rm bulk}$), respectively.

The Fermi energy is conventionally measured with respect to the valence band maximum (VBM) of the perfect supercell, $\epsilon_{\rm VBM}$. In this work, we adopted [20]

$$\epsilon_{\rm VBM} = E_{\rm tot}^{\rm perf}(q=0) - E_{\rm tot}^{\rm perf}(q=+1), \quad (4)$$

where $E_{\rm tot}^{\rm perf}(q)$ is the total energy of the perfect supercell in a charge state q. We employed uniform background charge distributions in the calculations for charged states to keep the charge neutrality over the supercells.

Because one-electron energy levels are displaced in calculations of periodic supercells with defects, the levels should be referenced back to the corresponding ones for the perfect crystal by an amount, ΔV,

$$\epsilon_{\rm F} = \epsilon_{\rm VBM} + \Delta V + \epsilon. \quad (5)$$

The shift ΔV can be obtained as the difference between the average electrostatic potential in the bulk-like region, which is the most distant plane from the defect in the supercell, and the corresponding one in the perfect supercell [21–24]. The conduction band minimum, $\epsilon_{\rm CBM}$, is defined by

$$\epsilon_{\rm CBM} = E_{\rm tot}^{\rm perf}(q=-1) - E_{\rm tot}^{\rm perf}(q=0). \quad (6)$$

The formation energy in equation (1), the difference between the total energy and the sum of the chemical potentials of constituent atoms and excess electrons, can be regarded as the energy required to generate the defect under a crystal growth condition.

In the limit of dilute concentrations, it is assumed that the defect concentration, $C_{\rm d}$, obeys the following distribution,

$$C_{\rm d}(\epsilon_{\rm F}, T) = N_{\rm d} \exp\left(-\frac{E_{\rm f}^{\rm d}}{k_{\rm B}T}\right), \quad (7)$$

where $N_{\rm d}$ is the concentration of the sublattice site relevant to the defect d. The Boltzmann's constant and the absolute temperature are denoted by $k_{\rm B}$ and T, respectively. The Fermi energy and defect concentrations are determined by the charge neutrality condition [25],

$$\sum_d q_{\rm d} C_{\rm d}(\epsilon_{\rm F}, T) = n(\epsilon_{\rm F}, T) - p(\epsilon_{\rm F}, T), \quad (8)$$

where the carrier densities, n and p, are the thermodynamically equilibrium electron and hole concentrations, which are expressed by

$$\mathrm{n}(\epsilon_{\rm F}, T) = \sum_{\epsilon_n > \epsilon_{\rm CBM}} f(\epsilon_n, \epsilon_{\rm F}, T) D_{\epsilon_n}, \quad (9a)$$

$$\mathrm{p}(\epsilon_{\rm F}, T) = \sum_{\epsilon_n < \epsilon_{\rm VBM}} [1 - f(\epsilon_n, \epsilon_{\rm F}, T)] D_{\epsilon_n}, \quad (9b)$$

where $f(\epsilon_n, \epsilon_{\rm F}, T)$ is the Fermi–Dirac distribution function and D_{ϵ_n} is the number of states with a one-electron energy, ϵ_n, in the perfect supercell.

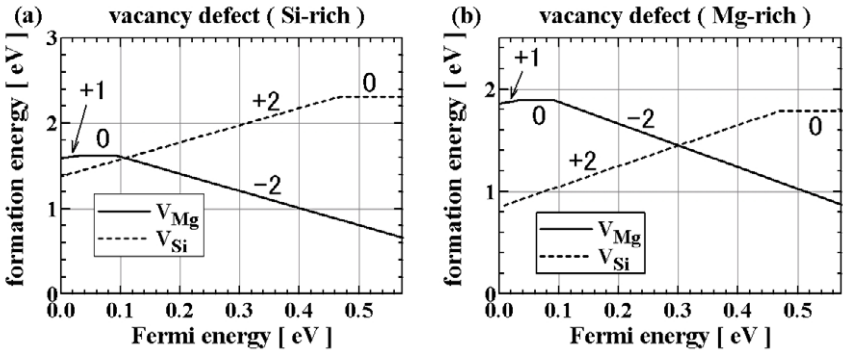

Figure 1. Formation energies for vacancy defects, V_{Mg} and V_{Si}, under (a) Si-rich and (b) Mg-rich conditions. The charge states with the lowest formation energies are depicted. The origin of Fermi energy is the corrected valence band maximum, $\epsilon_{VBM} + \Delta V$.

2.2. Born effective charge tensors

In order to examine the chemical bonding character in Mg_2Si, we calculate the Born effective charge tensors, Z_{ij}, by a conventional method [26],

$$Z_{ij}^{\alpha} = \frac{\partial P_i}{\partial \tau_j^{\alpha}} \sim \frac{\Delta P_i}{\Delta \tau_j^{\alpha}}, \tag{10}$$

where $\boldsymbol{P}$ is the polarization vector and $\Delta\tau^{\alpha}$ is the αth atom displacement-vector from the ideal coordinate. The subscripts stand for the Cartesian components. The Brillouin-zone integrations for the polarization calculations were carried out with regularly spaced $12 \times 12 \times 12$ points in the reciprocal unit-cell for the fcc primitive cell with one chemical formula. The differentiation in equation (10) is replaced by a finite difference scheme. We found at least $|\Delta\tau^{\alpha}| \sim 0.01$ Å provided a well converged Z_{ij}^{α}. The effective charge tensors calculated with these conditions satisfied a sum rule [27–29],

$$\sum_{\alpha} Z_{ij}^{\alpha} = 0, \tag{11}$$

to a precision of 0.01 per primitive cell in units of elementary charge, e.

3. Results and discussion

We obtained the following convergence properties by employing a cutoff energy for the wavefunction expansion, 30Hr. For the perfect unit-cell, we obtained the optimized lattice constant, 6.235 Å, which is in good agreement with the earlier theoretical result [30] and it is slightly (1.8%) smaller than the experimental results, 6.35 Å [31, 32]. The obtained value of $\Delta H_f^{Mg_2Si}$, which is defined in equation (2), is 0.528 eV, this is close to the previous GGA result of 0.52 eV [33].

As the reference perfect supercell, we employed a system, which contained 96 atoms ($n_{Mg} = 64$ and $n_{Si} = 32$). The Brillouin-zone integrations in the total energy calculations for supercells were carried out with a regular mesh of $2 \times 2 \times 2$ points in the reciprocal unit-cell for the supercell.

We obtained the conduction band minimum, ϵ_{CBM}, 0.57 eV above the valence band maximum, ϵ_{VBM}. The converged band gap energy, 0.19 eV, was obtained when we employed a sufficiently dense mesh for Brillouin-zone integrations and this is in good agreement with the earlier theoretical result [30]. The discrepancy is due to our coarse mesh points. Nevertheless, the calculated formation energies for major defects stayed almost unchanged (<0.01 eV) when we adopted a denser mesh ($4 \times 4 \times 4$). We made no corrections for the band gap because the magnitude of the band gap energy is still under investigation [34, 35].

3.1. Defect formation energies

We carried out self-consistent total energy calculations for defect supercells in variously charged states (from -4 to $+4$ in units of e). The inner coordinates of all atoms within a sphere of radius 6 Å around a relevant defect were relaxed until the maximum residual forces were less than 10^{-3} eV Å^{-1} with no imposed symmetries. The calculations with the relaxation-cutoff radius gave sufficiently converged total energies in reference to all-atom-relaxation results (<0.02 eV). We also confirm that the spin degree of freedom provides insignificant contributions (<0.01 eV) to the total energies for odd electron systems, such as Mg_i^{+}, Mg_i^{3+}, V_{Mg}^{-} etc.

Two kinds of point vacancy defects, V_{Mg} and V_{Si}, were examined. In figure 1, the lowest formation energies for V_{Mg} and V_{Si} are shown. A negatively charged defect, V_{Mg}, has low formation energies for the Si-rich condition as expected. It generates holes in the valence bands and should act as an acceptor. The Mg vacancy, V_{Mg}, is more favorable than V_{Si} except for a p-type environment (low Fermi energy region) and especially with a Si-rich condition. Moreover, V_{Mg} has lower formation energies under a Si-rich condition than under a Mg-rich condition. That is quite reasonable because a Si-rich condition is also referred to as a Mg-poor condition.

In the Mg_2Si crystal structure, only one type of interstitial site (**4b**) is possible and it is surrounded by eight Mg ions, so next two kinds of interstitial point defects, Mg_i and Si_i, were examined. The lowest formation energies for Mg_i and Si_i, are shown in figure 2. The present calculations indicate that Mg_i is energetically more favorable than Si_i over the whole band gap. It is reasonable to assume that the formation of Mg_i is more favorable under a Mg-rich condition than under a Si-rich condition. The positively charged defect, Mg_i, gives electrons in the conduction bands and should act as a donor.

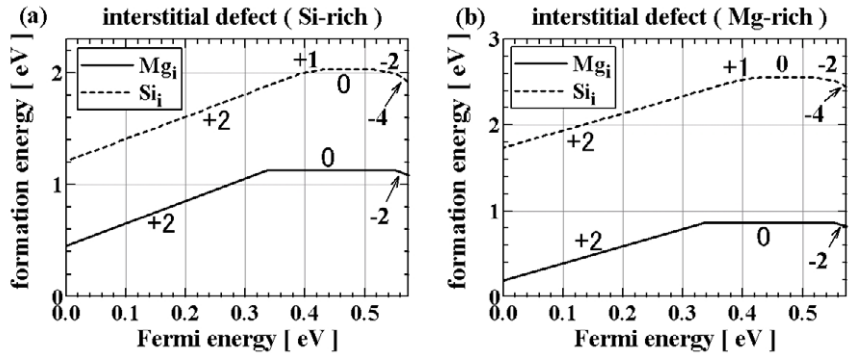

Figure 2. Formation energies for defects at the **4b** interstitial site, Mg_i and Si_i, under (a) Si-rich and (b) Mg-rich conditions. The charge states with the lowest formation energies are depicted. The origin of Fermi energy is $\epsilon_{VBM} + \Delta V$.

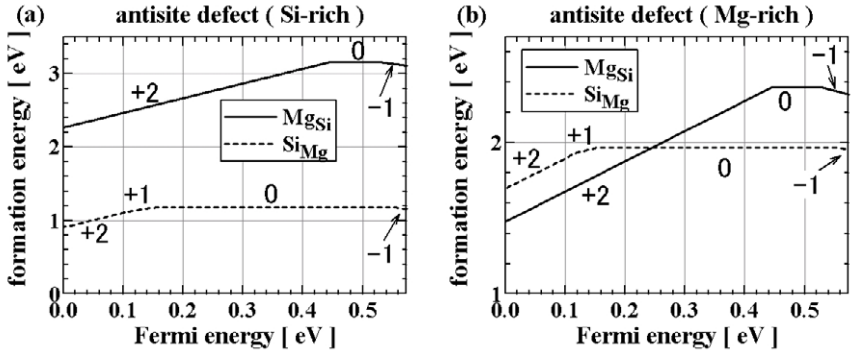

Figure 3. Formation energies for antisite defects, Mg_{Si} and Si_{Mg}, under (a) Si-rich and (b) Mg-rich conditions. The charge states with the lowest formation energies are depicted. The origin of Fermi energy is $\epsilon_{VBM} + \Delta V$.

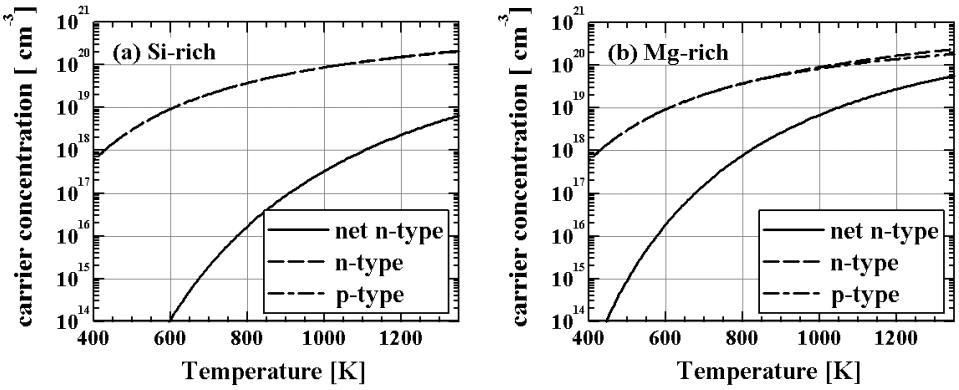

Figure 4. Carrier concentrations as functions of crystal growth temperature under (a) Si-rich and (b) Mg-rich conditions. The term, 'net n-type', stands for the difference between n- and p-type carrier concentrations.

The lowest formation energies for antisite defects, Mg_{Si} and Si_{Mg}, are shown in figure 3. In particular, Mg_{Si} is energetically unfavorable and that will be discussed in section 3.3 in terms of the ionic radii.

3.2. Carrier and defect concentrations

We calculated defect and carrier concentrations with Fermi energies by means of the charge neutrality condition, equation (8). Figure 4 shows the obtained carrier concentrations as functions of crystal growth temperature. The n-type carrier concentration slightly exceeds the p-type one under both off-stoichiometric conditions. In addition, the effective mass for an electron is smaller than the one for a hole [36], the result from the band structure of Mg_2Si. These facts indicate that Mg_2Si always exhibits n-type conductivity whether it is fabricated under Si-rich or Mg-rich conditions. Moreover, the net n-type carrier concentration under a Mg-rich condition is larger than the one under a Si-rich condition. The Fermi energies appear in figure 5. The Fermi energy for the Mg-rich condition is higher than that for the Si-rich condition. This is consistent with the above carrier concentration result.

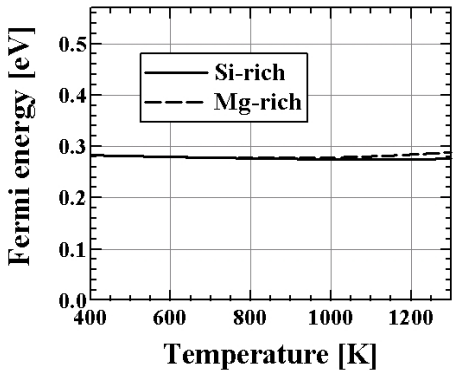

Figure 5. Fermi energies as functions of crystal growth temperature under Si-rich and Mg-rich conditions.

Figure 6 illustrates the major defect concentrations, which are the sum of the concentrations of the respective defects in all charge states. The concentrations of other types of defects are more than two orders of magnitude lower.

Figures 3 and 5 indicate that the major charge state of Si_{Mg} is neutral, so Si_{Mg} is less important with respect to the carrier generation mechanism. The concentration of Mg_i, which acts as a donor, is higher than the one for V_{Mg}, which acts as an acceptor, and the difference is larger under a Mg-rich condition than under a Si-rich one. That is why the net n-type carrier concentration for the Mg-rich condition is higher than the one for the Si-rich condition.

Figures 2 and 5 indicate that the major charge state of Mg_i is nominal, Mg_i^{2+}, under any chemical composition. Then the source of the persistent n-type conductivity of Mg_2Si is the formation of the positively divalent interstitial Mg defect as an donor; $Mg_i \rightarrow Mg_i^{2+} + 2e^-$.

We examined the validity of our supercell size by calculating the formation energies for major defects (Mg_i^{2+}, V_{Mg}^{2-}) with a larger supercell (324 atoms). The differences in the corresponding formation energies were 0.05 eV for Mg_i^{2+} and 0.02 eV for V_{Mg}^{2-}, respectively. Our conclusions stay unchanged against increasing supercell size because the differences show little change from figures 1 and 2.

Moreover we verified the reliability of the method we used here by applying it to pure bulk silicon (the reference perfect supercell contains 64 atoms). As the result of our calculation, the net carrier concentration is quite low even at high temperatures, *e.g.* 1.4×10^{13} cm^{-3}, whereas n $\sim$ p $\sim$ 6×10^{19} cm^{-3} at 1500 K. That is qualitatively reasonable because a large compensation between n and p in pure bulk silicon is widely accepted. However it should be noted that carrier concentrations, n and p $\sim 1.4 \times 10^{16}$ cm^{-3} at 500 K, are overestimated when compared to an experimental result, 10^{14-15} cm^{-3} at 500 K [37]. Rigorous quantitative checks should be done with larger supercells and with a band gap correction.

3.3. Born effective charge tensors and bonding characterization

We examined the bonding character of Mg_2Si in terms of Born effective charge tensors. Generally, Born effective charge tensors in ionic crystals are almost diagonal and the values of the diagonal elements are close to their nominal valence numbers. In contrast, covalent bondings produce off-diagonal elements and the values of diagonal elements deviate far from their nominal ones [28, 29].

The calculated Born effective charge tensors for Mg and Si in a Mg_2Si perfect crystal are as follows,

$$Z^{Mg} = \begin{pmatrix} +1.84 & 0.00 & 0.00 \\ 0.00 & +1.84 & 0.00 \\ 0.00 & 0.00 & +1.84 \end{pmatrix}, \qquad (12a)$$

$$Z^{Si} = \begin{pmatrix} -3.67 & 0.00 & 0.00 \\ 0.00 & -3.67 & 0.00 \\ 0.00 & 0.00 & -3.67 \end{pmatrix}. \qquad (12b)$$

Both effective charge tensors are almost diagonal and the magnitudes of the diagonal elements are close ($\sim$92%) to the nominal valence numbers of the ions. This suggests that the bonding character in Mg_2Si is ionic, thus their ionic radii are expected to be well-defined.

The total valence charge density distribution for the perfect crystal is shown in figure 7. It shows close similarity to the earlier theoretical result [30] and exhibits fairly the ionic charge density distribution, as expected from the calculated Born effective charge tensors. Furthermore, the distribution

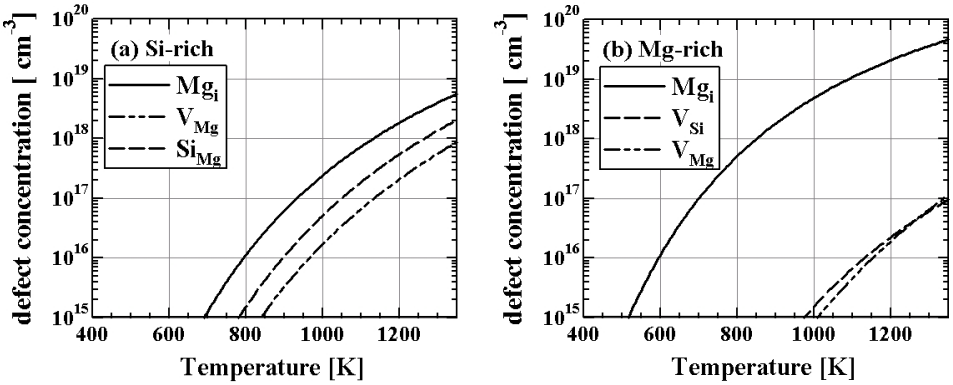

Figure 6. Concentrations of major defects, Mg_i and V_{Mg}, as functions of crystal growth temperature under (a) Si-rich and (b) Mg-rich conditions.

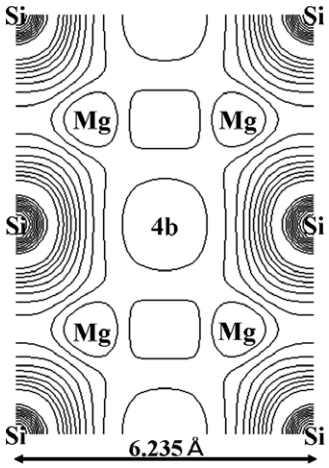

Figure 7. Total valence charge density distribution of (110) plane of Mg_2Si. The symbols, 'Mg' and 'Si' denote the position of the center of respective ions and '**4b**' stands for the interstitial site.

indicates a significant difference in ionic radius between Mg^{2+} and Si^{4-}. We estimated the ionic radius for Mg^{2+}, $r_{Mg^{2+}}$, at 0.6 Å and that for Si^{4-}, $r_{Si^{4-}}$, at 2.1 Å, by regarding the boundary between Mg^{2+} and Si^{4-} as the isodensity surface extending across both ions. The ionic radius, $r_{Mg^{2+}}$ is in good agreement with the widely-accepted empirical value, 0.58 Å [38], as the radius of the divalent Mg cation at a tetrahedral site. The ionic radius, $r_{Si^{4-}}$, is about three times larger than $r_{Mg^{2+}}$. In general, antisite defects have high formation energies if the mutual ionic radii are markedly dissimilar [39]. That agrees with our result in section 3.1, i.e., the antisite defect, Mg_{Si} is energetically unfavorable.

In contrast, Si_{Mg}, the other type of antisite defect, reveals a relatively high defect concentration in a Si-rich condition (figure 6). Figures 3 and 5 indicate the major charge state of Si_{Mg} is neutral, Si^0_{Mg}. This suggests that the Si ion at a Mg-site is a divalent *cation*, Si^{2+}, in Si^0_{Mg}. In general, a cation has a smaller ionic radius than the anions of the same element. Then the difference between the ionic radii should be reduced. That is why Si_{Mg} reveals a higher defect concentration than Mg_{Si}. It should be noted that Si_{Mg} gives a minor contribution to carrier generation because the major charge state is neutral.

4. Conclusions

We have investigated the intrinsic point defect formations in Mg_2Si by density-functional theory and have elucidated that the donor-like Mg_i is a major defect and the persistent n-type conductivity originates from excess n-type carriers from Mg_i, whatever chemical composition the crystal is grown under. The net n-type carrier concentration is much higher under a Mg-rich condition than under a Si-rich condition. These results are consistent with experimental results; Mg_2Si exhibits persistent n-type conductivities [1, 7] and the crystal which is grown under a Mg-rich condition exhibits higher electric conductivity than the one grown under a Si-rich condition [8].

The antisite defect, Mg_{Si}, requires higher formation energies compared with major defects, Mg_i. Thus Mg_{Si} is a minority (less than 10^{15} cm^{-3}) in Mg_2Si. The Born effective charge tensors exhibit the ionic bonding between positively divalent Mg and negatively quadrivalent Si. Furthermore, the valence charge density distribution shows that their ionic radii are quite different (0.6 Å for Mg^{2+} and 2.1 Å for Si^{4-}). It is reasonable to assume that highly charged anions (Si^{4-}) have large ionic radii and that the antisite defects, Mg_{Si}, relevant to the ions with dissimilar radii, have high formation energies.

Though we assume thermodynamic equilibrium conditions in crystal growth processes instead of dealing with explicit dynamics, high mobilities of Mg in Mg_2Si, which have been reported in earlier experiments [13, 14], allow defect formations associated with Mg to reach thermodynamic equilibrium in crystal growth. Therefore, it can be said that our results make sense because Mg_i is identified as the major defect in our calculations.

Acknowledgments

We gratefully acknowledge Professor H Tatsuoka (Shizuoka University), K Hakamata, and M Mouri for fruitful discussion.

References

[1] Heller M W and Danielson G C 1962 *J. Phys. Chem. Solids* **23** 601
[2] Akasaka M, Iida T, Matsumoto A, Yamanaka K, Takanashi Y, Imai T and Hamada N 2008 *J. Appl. Phys.* **104** 013703
[3] Nolas G S, Wang D and Beekman M 2007 *Phys. Rev.* B **76** 235204
[4] Aoyama I, Kaibe H, Rauscher L, Kanda T, Mukoujima M, Sano S and Tsuji T 2005 *Japan. J. Appl. Phys.* **44** 6A 4275
[5] Goranova E, Amov B, Baleva M, Trifonova E P and Yordanov P 2004 *J. Mater. Sci.* **39** 1857
[6] Vantomme A, Mahan J E, Langouche G, Becker J P, Bael M V, Temst K and Haesendonck C V 1997 *Appl. Phys. Lett.* **70** 1086
[7] Morris R G, Redin R D and Danielson G C 1958 *Phys. Rev.* **109** 1909
[8] Yoshinaga M, Iida T, Noda M, Endo T and Takanashi Y 2004 *Thin Solid Films* **461** 86
[9] Shanks H R 1974 *J. Cryst. Growth* **23** 190
[10] Imai Y, Watanabe A and Mukaida M 2003 *J. Alloys Compounds* **358** 257
[11] Van de Walle C G, Laks D B, Neumark G F and Pantelides S T 1993 *Phys. Rev.* B **47** 9425
[12] Van de Walle C G and Neugebauer J 2004 *J. Appl. Phys.* **95** 3851
[13] Chu W K, Lau S S, Mayer J W, Müller H and Tu K N 1975 *Thin Solid Films* **25** 393
[14] Takagi N, Sato Y, Matsuyama T, Tatsuoka H, Tanaka M, Fengmin C and Kuwabara H 2005 *Appl. Surf. Sci.* **244** 330
Mizuyoshi Y, Yamada R, Ohishi T, Saito Y, Koyama T, Hayakawa Y, Matsuyama T and Tatsuoka H 2006 *Thin Solid Films* **508** 70
[15] Kato A and Rikukawa H 2005 *Phys. Rev.* B **72** 041101(R)
[16] Hohenberg P and Kohn W 1964 *Phys. Rev.* **136** B864
Kohn W and Sham L J 1965 *Phys. Rev.* **140** A1133
[17] Hartwigsen C, Goedecker S and Hutter J 1998 *Phys. Rev.* B **58** 3641
Goedecker S, Teter M and Hutter J 1996 *Phys. Rev.* B **54** 1703
[18] Qian G-X, Martin R M and Chadi D J 1988 *Phys. Rev.* B **38** 7649
[19] Fukumoto A 1996 *Phys. Rev.* B **53** 4458

[20] Togo A, Oba F, Tanaka I and Tatsumi K 2006 *Phys. Rev.* B **74** 195128
[21] Balderschi A, Baroni S and Resta R 1988 *Phys. Rev. Lett.* **61** 734
[22] Laks D B, Van de Walle C G, Neumark G F, Blöchl P E and Pantelides S T 1992 *Phys. Rev.* B **45** 10965
[23] Garcia A and Northrup J E 1995 *Phys. Rev. Lett.* **74** 1131
[24] Pöykkö S, Puska M J and Nieminen R M 1996 *Phys. Rev.* B **53** 3813
[25] Zhang S B and Northrup J E 1991 *Phys. Rev. Lett.* **67** 2339
[26] Resta R 1994 *Rev. Mod. Phys.* **66** 899
[27] Gonze X and Lee C 1997 *Phys. Rev.* B **55** 10355
[28] Posternak M, Resta R and Baldereschi A 1994 *Phys. Rev.* B **50** 8911
[29] Miwa K, Ohba N, Towata S, Nakamori Y and Orimo S 2004 *Phys. Rev.* B **69** 245120
[30] Benhelal O, Chahed A, Laksari S, Abbar B, Bouhafs B and Aourag H 2005 *Phys. Status Solidi* b **242** 2022
[31] Nikitin E N, Tkalenko E N, Zaitsev V K, Zaslavskii A I and Kuznetsov A K 1968 *Inorg. Mater. USSR* **4** 1656
[32] Mahan J E, Vantomme A, Langouche G and Becker J P 1996 *Phys. Rev.* B **54** 16965
[33] Imai Y and Watanabe A 2002 *Intermetallics* **10** 333
[34] Arnaud B and Alouani M 2000 *Phys. Rev.* B **62** 4464
Arnaud B and Alouani M 2001 *Phys. Rev.* B **64** 033202
[35] Tamura D, Nagai R, Sugimoto K, Udono H, Kikuma I, Tajima H and Ohsugi I J 2007 *Thin Solid Films* **515** 8272
[36] Zaitsev V K, Fedorov M I, Gurieva E A, Eremin I S, Konstantinov P P, Samunin A Yu and Vedernikov M V 2006 *Phys. Rev.* B **74** 045207
[37] Pierret R F 1996 *Semiconductor Device Fundamentals* (Reading, MA: Addison-Wesley)
[38] Shannon R D 1976 *Acta Crystallogr.* A **32** 751
[39] Neugebauer J and Van de Walle C G 1994 *Phys. Rev.* B **50** 8067